# NACA

# RESEARCH MEMORANDUM

for the

U. S. Air Force

FREE-FLIGHT TESTS OF 1/9-SCALE CONVAIR YF-102 AIRPLANE

WINGS AT TRANSONIC AND SUPERSONIC SPEEDS TO

INVESTIGATE THE POSSIBILITY OF FLUTTER

By Burke R. O'Kelly

Langley Aeronautical Laboratory
Langley Field, Va.

# NATIONAL ADVISORY COMMITTEE
# FOR AERONAUTICS
## WASHINGTON

OCT 4 1955

14

NATIONAL ADVISORY COMMITTEE FOR AERONAUTICS

RESEARCH MEMORANDUM

for the

U. S. Air Force

FREE-FLIGHT TESTS OF 1/9-SCALE CONVAIR YF-102 AIRPLANE

WINGS AT TRANSONIC AND SUPERSONIC SPEEDS TO

INVESTIGATE THE POSSIBILITY OF FLUTTER

By Burke R. O'Kelly

SUMMARY


Free-flight tests in the transonic and supersonic speed ranges uti-
lizing rocket-propelled models have been made on two pairs of 1/9-scale
Convair YF-102 airplane wings with elevons to investigate the possibility
of flutter. These wings had modified 60° delta plan forms with the
trailing edge swept forward 5°. The aspect ratio of two exposed wing
panels was 2.19 and the wings had NACA 0004-65 (modified) airfoil sections.
The model wings and elevons were dynamic-scale models at sea level of the
full-scale wings at 20,000 feet.

The first set of wings developed elevon buzz near a Mach number of 1
during both power-on and coasting flight at amplitudes of equal to or
greater than ±4°. The second set of wings did not develop the elevon
buzz experienced by the first set but, as the model reached the maximum
speed of the test (Mach number 1.93), one or both of the wings suddenly
failed, possibly as a result of aerodynamic heating or high stresses
imposed on the wings at separation from the booster. No flutter was
experienced during either flight.

INTRODUCTION


At the request of the Air Force, free-flight rocket-propelled-model
tests at transonic and supersonic speeds have been conducted by the
Langley Laboratory to investigate the possibility of flutter of 1/9-scale
Convair YF-102 airplane wings. This paper presents the results of the
first two tests of a series. The test wings were dynamic models of the
full-scale wing and were equipped with spring-restrained elevons. The
model wings, tested near sea level, simulated the full-scale wings at
20,000 feet. The first model was tested to a maximum Mach number of 1.31
to investigate the possibility of flutter in the transonic and low super-
sonic speed range. The second model was tested to a Mach number of 1.93
to explore the possibility of flutter at higher supersonic speeds.

## SYMBOLS

$A_{ex}$        aspect ratio of two exposed wing panels

$a_n/g$        model normal accelerometer reading

$f$        frequency, cps

$M$        Mach number

$S_{ex}$        area of two exposed wing panels, sq ft

$t$        time from launching, sec

$V$        velocity, fps

$\delta$        elevon deflection, deg

$\rho$        atmospheric density, slugs/cu ft

## MODELS AND INSTRUMENTATION

### Models

The test vehicle used in this investigation was a cylindrical body with a parabolic nose. The test wings were mounted in an aluminum-alloy casting which was a structural part of the body. An oversize slot in each side of the casting received the undersize root attachment of each wing and bolts were installed to hold the wing in place. A thermosetting polyester resin was used to fill the spaces between the root attachment and the walls of the slot. Past experience has shown that this procedure results in a mounting which has more than adequate strength. Two vertical fins were attached to provide directional stability and stability in pitch was provided by the test wings.

The lower speed model ($M \leqq 1.3$) contained a 5-inch cordite rocket motor which, after model-booster separation, accelerated the model at about 8g through the flutter test range. The higher speed model ($M \leqq 1.93$) used a high-performance air-to-ground (HPAG) rocket motor modified to three-fourths of its original length to accelerate the model through the flutter test range at about 20g. The lower speed model used an HPAG rocket motor booster to accelerate the model to a Mach number of 0.76 and the higher speed model used a Deacon rocket motor booster which provided a Mach number of 1.27 at separation.

The general layout of the models is shown in figure 1 and a photo-
graph of one of the models is shown as figure 2(a). A photograph of the
higher speed model with its booster on the launcher is shown as figure 2(b).

Weight and balance data for the models are presented in table I.

Test Wings

Two pairs of Convair YF-102 flutter wings have been tested in this
investigation. The wings were 1/9-scale dynamic models of the full-scale
wings and had modified delta plan forms with the leading edge swept back
60° and the trailing edge swept forward 5°. The wings had an aspect
ratio of 2.19 and NACA 0004-65 (modified) streamwise airfoil sections.
A sketch of the wings giving pertinent dimensions is shown in figure 3(a).

The wings were dynamically scaled models equivalent at sea level to
the full-scale wings at 20,000 feet. Similarity requirements were based
on unity ratios of reduced frequency, mass ratio, Mach number, and struc-
tural damping. In order to meet these requirements, the model wing
structure was built up of ribs, spars, and skin. The structural charac-
teristics of the test wing were scaled down from the prototype according
to the ratios listed in table II. The components of the test wings were
bonded together with an adhesive because the usual method of fastening
with rivets was not feasible. Two dummy spars were built into the model
wings as a precaution against skin-panel flutter. The structure of the
elevon, because of its small size, was not duplicated on the model.
Instead the elevon was made of a balsa core having hardwood pads at the
places of attachment and covered with a thin (0.012 in.) aluminum skin.
Flexure pivots (fig. 4(a)) were used as the method of attachment rather
than hinges because of the possibility of binding in the hinges. Leaf
springs attached between the elevons and the wings simulated the torsional
stiffness of the elevon actuator and were designed to provide the scaled
rotational frequency of 243 cps. In order that the mass distribution of
the model and full-scale wings would be comparable, lead weights of the
proper amount were fastened in the wings in the proper places. A photo-
graph of the wing structure with the skin and elevon removed showing the
ribs, spars, weights, and flexure pivots is shown in figure 4(b).

Prior to the flight tests, the models were vibrated in the labora-
tory and the natural frequencies and node lines of the wings were recorded
and are shown in figure 5. Each model was suspended by shock cord at its
center of gravity where it was vibrated by an electrodynamic shaker.
Although the wings were fabricated alike, the wing frequencies and node
line locations varied widely between models 1 and 2. The natural rota-
tional frequency of the elevons could not be found, even though there
were node lines close to the elevon hinge line at 240 cycles per second
on model 1 and at 222 and 236 cycles per second on model 2. Comparisons
of the scaled measured frequencies of the full-scale wings with the

measured frequencies of the scaled wings mounted on the models is shown in table III. Frequencies and node lines for the full-scale wings may be seen in reference 1.

Structural influence coefficients for one set of the wings were measured by Convair and are given in reference 2. These influence coefficients were normalized, averaged, and corrected for flexibility of the root attachment by Convair. Calculated influence coefficients for the full-scale wing were scaled to model values and, when compared with values obtained from the model, were considered to be in reasonable agreement.

## Instrumentation

The models were equipped with telemeters which gave continuous records of the quantities to be measured. These quantities for both models were normal acceleration of each wing provided by vibrometers installed as shown in figure 3, normal acceleration near the model center of gravity, and total pressure. Also measured were deflection of the right-wing elevon for model 1 and deflection of the left-wing elevon for model 2.

The vibrometer is an accelerometer designed to give a true representation of frequency. No reliance can be placed on the values of acceleration from the vibrometers. Atmospheric conditions prevailing at the times of the model flights were obtained from radiosondes. Each radiosonde was tracked during its ascent by radar to determine the wind velocity. Two radar sets tracked the models during their flights; one to give the relative velocity of the models with respect to a ground reference point and the other to give their positions in space. The models were tracked by motion-picture cameras to give photographic records of the flights. They were launched at the Langley Pilotless Aircraft Research Station at Wallops Island, Va.

## FLIGHT TEST RESULTS

Time histories of the flights showing Mach number, velocity, and atmospheric density are shown in figure 6. Portions of the telemeter records are reproduced in figure 7 and portions of the data reduced from the telemeter records are shown in figure 8.

## Model 1

Figures 7(a) and 8(a) show vibrations of the elevons beginning at $M = 1.05$ ($V = 1160$ feet per second) having deflections with limits of $5^{\circ}$

and in excess of -2.7° at frequencies between 200 and 243 cycles per second. This vibration began to drive the wings and fuselage at the same frequency as the elevons. The vibrations stopped at M = 1.22 (V = 1335 feet per second). After the model reached maximum velocity (M = 1.31, V = 1440 feet per second) and was decelerating, the elevon vibrations began again at M = 1.08 (V = 1174 feet per second) having deflections with limits of nearly 6° and in excess of -2.7° at frequencies between 213 and 182 cycles per second. The wings began to vibrate almost immediately at the same frequency as the elevons and the model started to vibrate shortly thereafter. The open portions in the envelope of the elevon position (δ) curve of figure 8(a) indicate that the deflections read from the telemeter record were beyond the instrument calibration range. The magnitude of that portion of the envelope which is shown is in error to some extent owing to the attenuation in the instrumentation and no attempt should be made to establish a mean line. The vibrations stopped at M = 0.96 (V = 1050 feet per second). Normal loads on the model did not exceed the range of 3g to -2g during the vibrations. It is of interest to note that the elevons of the full-scale airplane buzzed at a Mach number slightly higher than 1 and at amplitudes of about ±0.3°.

## Model 2

Figure 8(b) shows that at about 1.8 seconds (M = 0.70, V = 780 feet per second) the model-booster combination began experiencing a steady increase in normal acceleration and that δ was increasing positively. At about 2.25 seconds (M = 0.92, V = 1030 feet per second), δ began to increase in the negative direction. As the Mach number increased to the maximum before booster separation (M = 1.26, V = 1411 feet per second), δ reached -0.7° and the normal acceleration reached 8.4g which amounted to about 2420 pounds of lift on the 288-pound combination. This load is about 940 pounds on the model alone. The design critical loading for the model was 1144 pounds (10.25g) based on calculations using a symmetrical step gust of 30 feet per second. The load encountered by the model, therefore, was 82.2 percent of this critical load. The model pitched rather severely after booster separation but damped rapidly. During sustainer burning the model oscillated about a trim line of about -0.4g with amplitudes of ±0.8g. As the model reached maximum velocity (M = 1.93, V = 2145 feet per second), the left wing suddenly failed (fig. 7(c)), the model became unstable, and thus the useful portion of the flight was ended. The vibrometer traces throughout the flight were similar in appearance to the traces shown in figure 7(c) before the failure of the wings.

It is possible that this failure might be the result of the structure of the wing having changed because of either the near design critical loads experienced at booster separation or as a result of softening of the adhesive bond due to high temperatures on the wing or for both

reasons. The temperature at a locus of points 6 inches back of the leading edge was calculated to be about 260° F at 6.7 seconds after launching based on the flight path that the model traversed. Owing to these conditions, further flutter tests on these wings at higher Mach numbers will be necessary.

## CONCLUDING REMARKS

There was no indication of wing flutter during the tests up to a Mach number of 1.31 for one model and a Mach number of 1.93 for the other. Although no wing flutter occurred during either flight, elevon vibrations or buzz occurred on the first model at frequencies of from 182 to 243 cycles per second having deflections with limits of 6° and in excess of -2.7° over Mach number ranges of 1.05 to 1.22 during accelerating flight and 1.08 to 0.96 during coasting flight.

Two possible explanations for the failure which occurred on the wings of the second model are weakening of the wings from the high loads imposed at booster separation and softening of the adhesive bond at the temperatures encountered by the model so that the wings were weakened or both.

Langley Aeronautical Laboratory,
        National Advisory Committee for Aeronautics,
                Langley Field, Va., December 8, 1954.

                                        Burke R. O'Kelly
                                        Aeronautical Research Scientist

Approved:
                Joseph A. Shortal
        Chief of Pilotless Aircraft Research Division

sam

## REFERENCES

1. Dublin, M., and Morgan, H.: Results of Ground Vibration Tests on the YF-102 Airplane. Rep. No. ZU-8-011 (Contract AF33(600)-5942), Consolidated Vultee Aircraft Corp., Nov. 2, 1953.

2. Wolfe, J. J., and Camp, R. G.: 1/9 Scale Flutter Model Proof and Influence Coefficients Tests. Rep. No. 7839, Consolidated Vultee Aircraft Corp., Apr. 30, 1954.

TABLE I.- WEIGHT AND BALANCE DATA OF MODELS

|                                                      | Model 1 | Model 2 |
|------------------------------------------------------|---------|---------|
| Weight with fuel, lb . . . . . . . . . . . . . . . . | 159.0   | 149.5   |
| Weight without fuel, lb . . . . . . . . . . . . . .  | 132.75  | 111.75  |
| Wing loading with fuel, lb/sq ft . . . . . . . . .   | 28.3    | 26.6    |
| Wing loading without fuel, lb/sq ft . . . . . . . .  | 23.6    | 19.8    |
| Center-of-gravity station with fuel, in. . . . .     | 52.41   | 52.41   |
| Center-of-gravity station without fuel, in. . . .    | 50.88   | 51.18   |
| Weight of each wing panel, lb . . . . . . . . . .    | 12.75   | 12.63   |

CONFIDENTIAL NACA RM SL54L22

TABLE II.- SIMILARITY REQUIREMENTS

| Quantity | Model value / Full-scale value |
|---|---|
| Strouhal number, $bf/V$ . . . . . . . . . . . . . . . . | 1 |
| Density ratio, $\rho b^3/m$ . . . . . . . . . . . . . . . . | 1 |
| Mach number, $V/V_c$ . . . . . . . . . . . . . . . . | 1 |
| Structural damping coefficient, g . . . . . . . . . | 1 |
| Length, b . . . . . . . . . . . . . . . . . . . . . | 1/9 |
| Mass, m . . . . . . . . . . . . . . . . . . . . . . | 1/387 |
| Mass moment of inertia, $I_\beta$ . . . . . . . . . . | 1/31,400 |
| Frequency, f . . . . . . . . . . . . . . . . . . . | 9.72 |
| Bending stiffness, EI . . . . . . . . . . . . . . . | 1/2990 |
| Torsional stiffness, GJ . . . . . . . . . . . . . . | 1/2990 |
| Skin or web thickness, t . . . . . . . . . . . . . | 1/4.1 |
| Stagnation pressure, q . . . . . . . . . . . . . . | 2.2 |
| Stress due to aerodynamic force, $\sigma_a$ . . . . . . . | 1 |
| Stress due to inertia force, $\sigma_i$ . . . . . . . . . | 1 |
| Deflection due to unit load, $\delta$ . . . . . . . . . | 4.1 |
| Deflection due to comparable loads, $\Delta$ . . . . . . | 1/9 |
| Elevon spring constant, k . . . . . . . . . . . . . | 1/333 |

TABLE III.- COMPARISON OF SCALED-FULL-SCALE-WING FREQUENCIES

WITH MODEL-WING FREQUENCIES

| Symmetrical mode | 9.72 full-scale frequency, cps | Model 1 frequency, cps | Model 2 frequency, cps |
|---|---|---|---|
| 1 | 96 | 81 | 76 |
| 2 | 165 | 104 | 100 |
| 3 | 202 | 118 | 108 |
| 4 | 232 | 144 | 124 |
| 5 | 282 | 205 | 168 |
| 6 | 382 | 223 | 222 |
| 7 | | 240 | 236 |
| 8 | | 320 | 298 |

Sta.0

39.72

85.5

7.0

9.0

12.76

Wing fence

$A_{ex}$ - 2.19

$S_{ex}$ - 5.60

4.0

2.5

52.5°

9.25

5.0

8.0

Side view of vertical fin
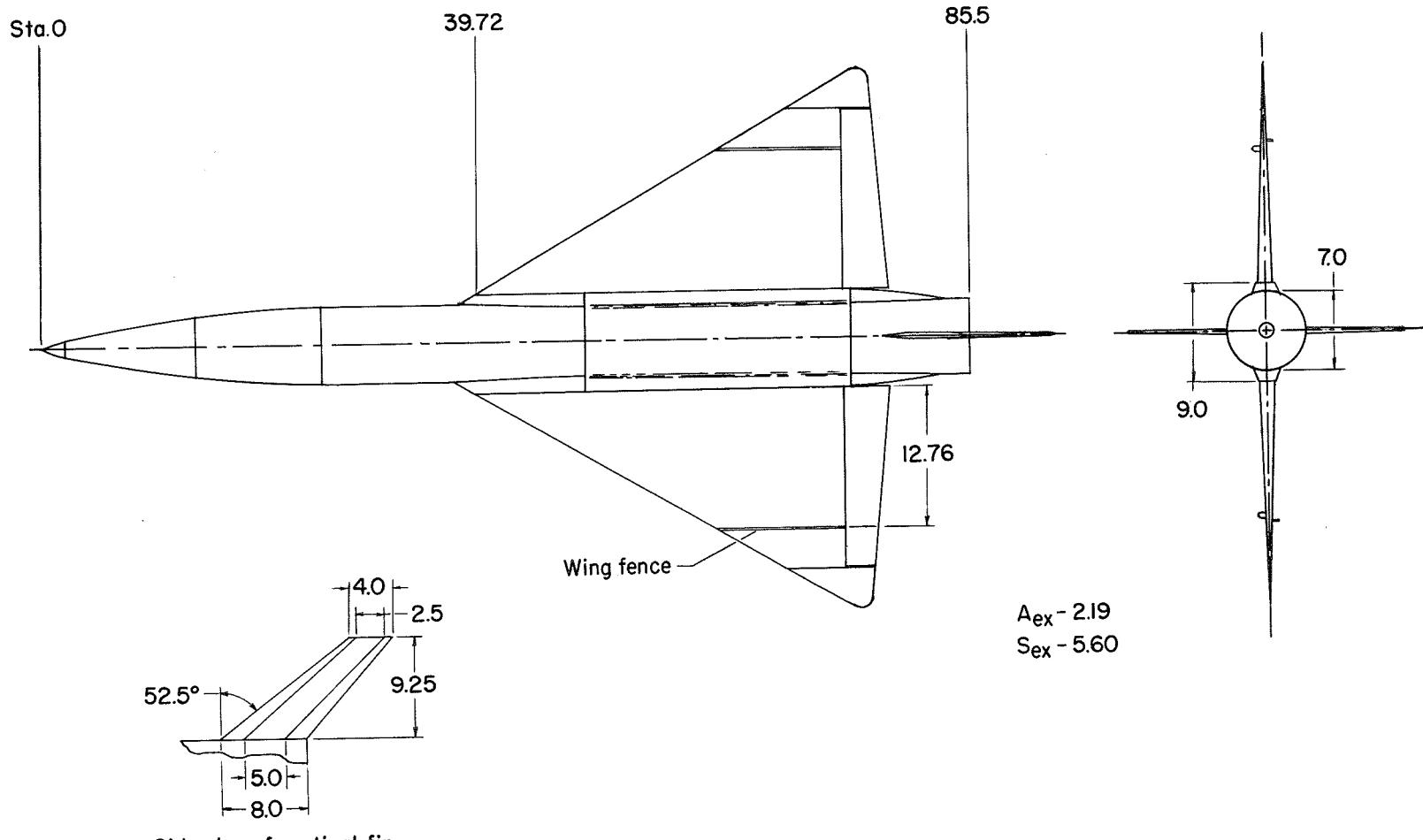
Figure 1.- General arrangement of the models.  All dimensions are in inches.
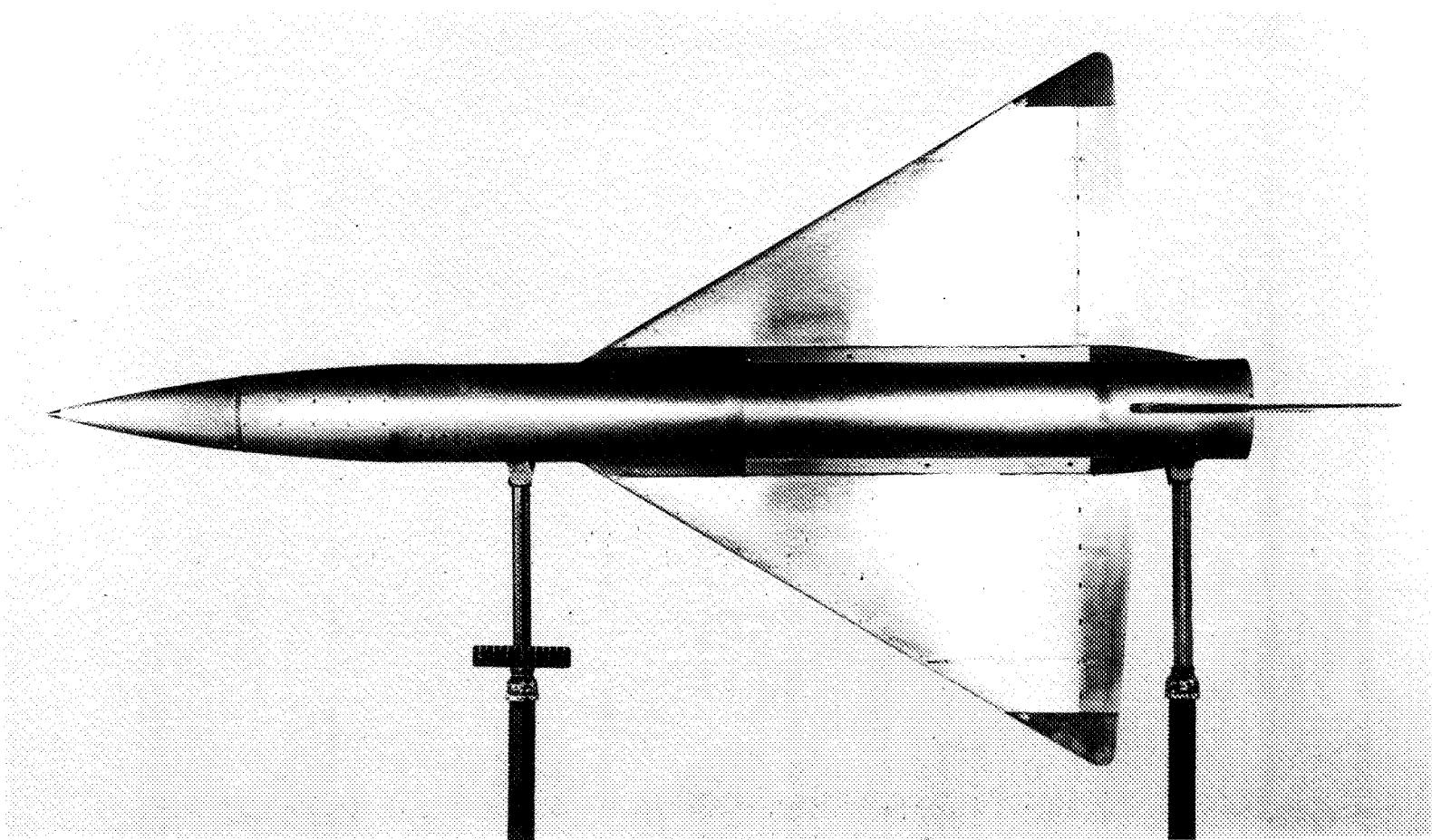
(a) Model 1.

L-84670.1

Figure 2.- Photographs of the models.
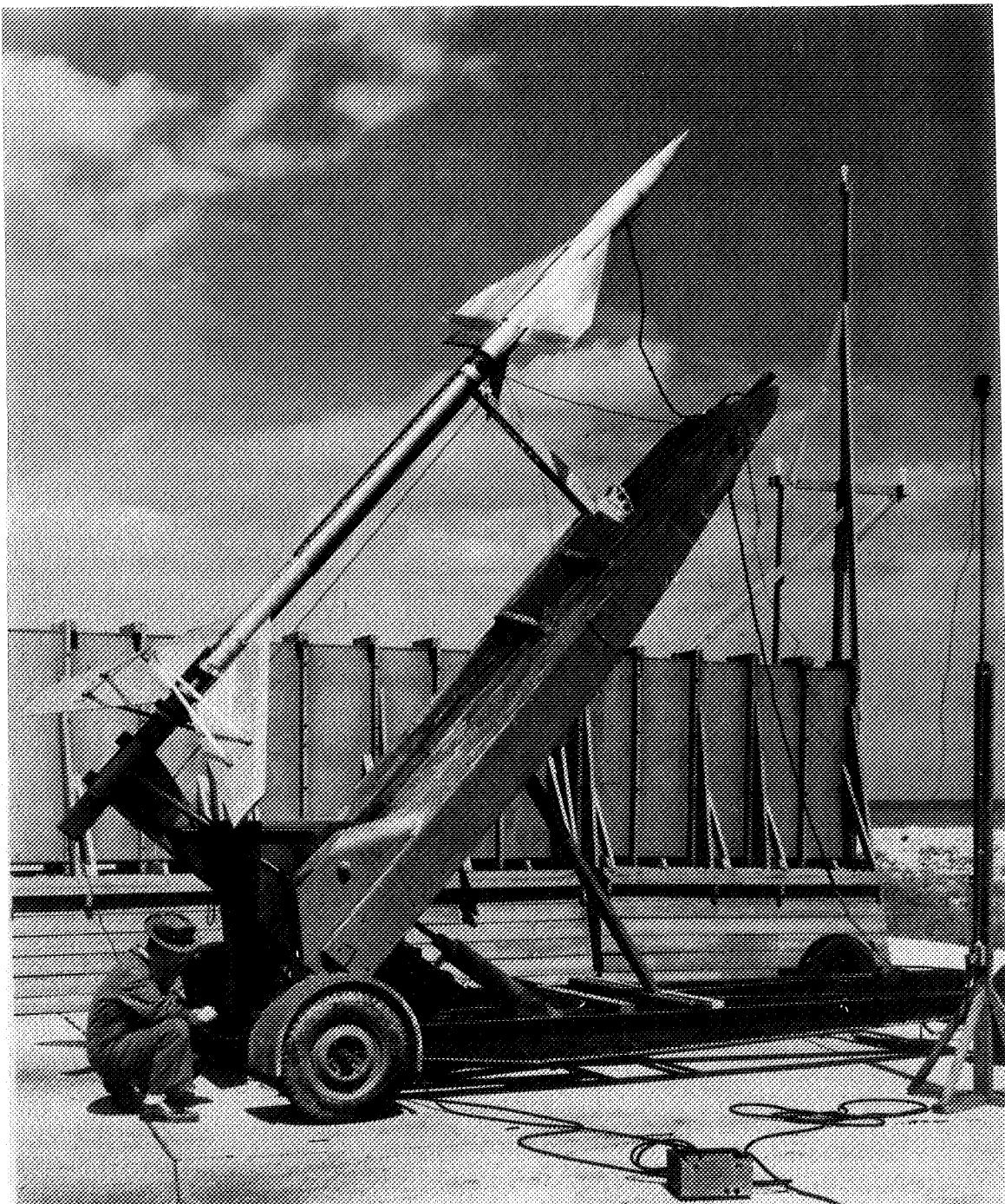
(b) Model 2 and booster on launcher.          L-85012.1

Figure 2.- Concluded.

Sta. 73.9

Projected tip

1.125 rad.

Unused vibrometer space

Dummy actuator fairing

21.06

2.71

24.11

Vibrometer door

16.44

12.33

11.0

60°

5°

3.25

4.5

8.78

Instrument
wiring tube

4.15

23.5

0.76

38.32

Model ℄

Root attachments

Landing gear door

Holes for mounting bolts

Elevon pick-up door
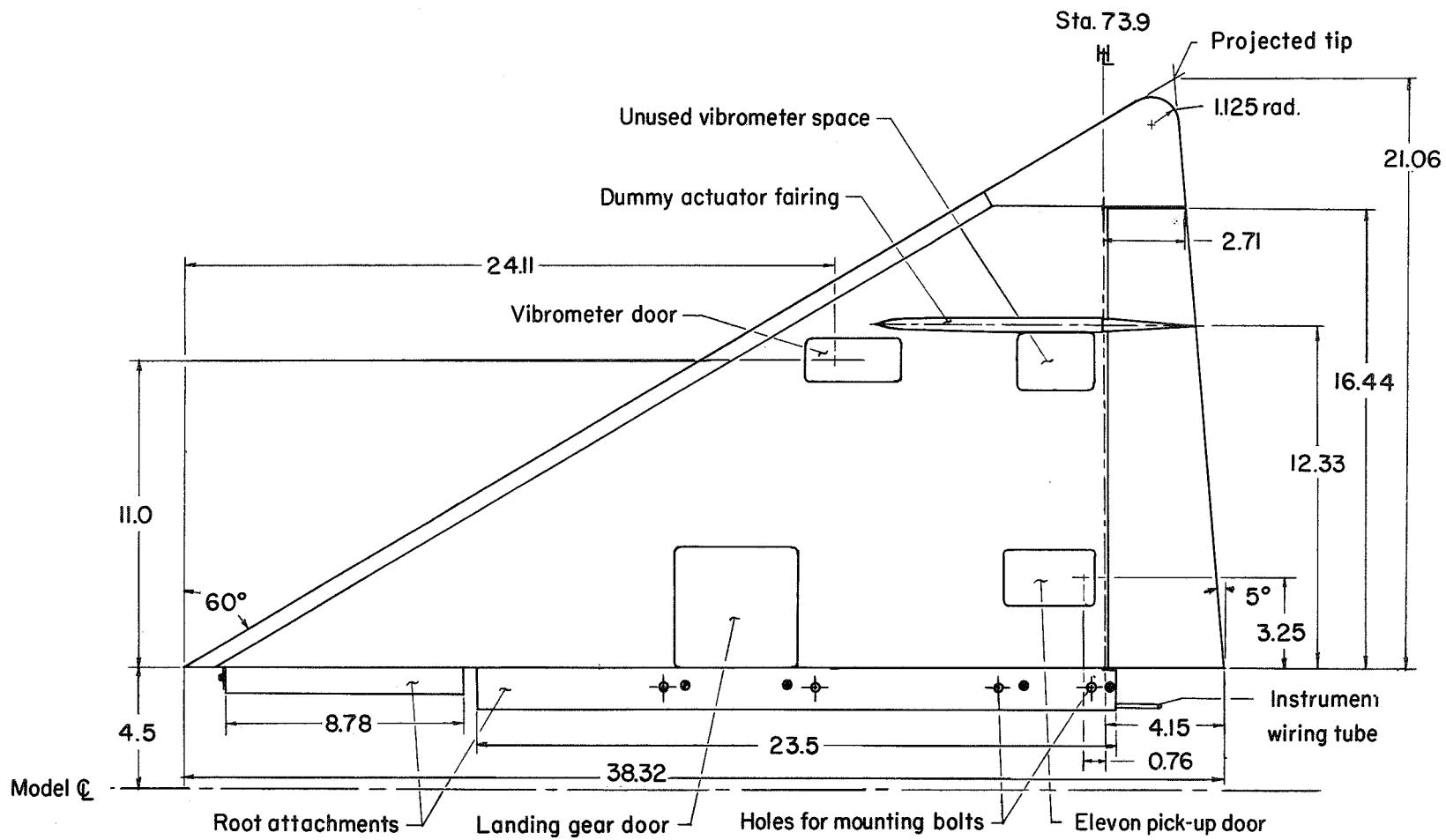
Figure 3.- Sketch of wing, underside view.  All dimensions are in inches.

Balsa core

Mahogany mounting pad
(I per pivot)

Aluminum skin
(0.012 inch thick)

Beryllium copper
flexure pivot
(5 per wing)

This surface screwed
to wing spar
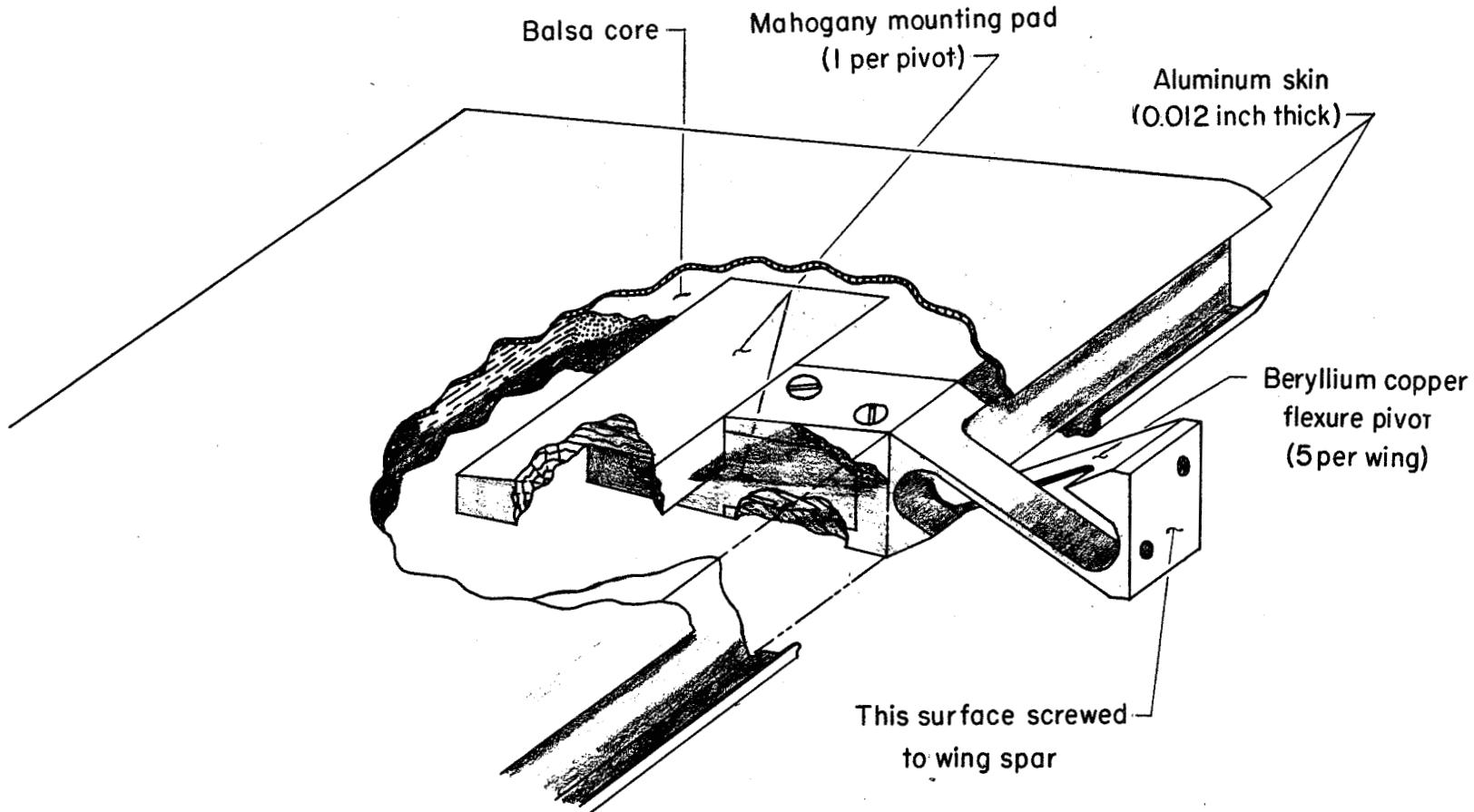
(a) Elevon and flexure pivot details.

Figure 4.- Wing and elevon structure.

Flexure pivots

Vibrometer mount

Lead weights

Vibrometer mount

Elevon position recorder mount
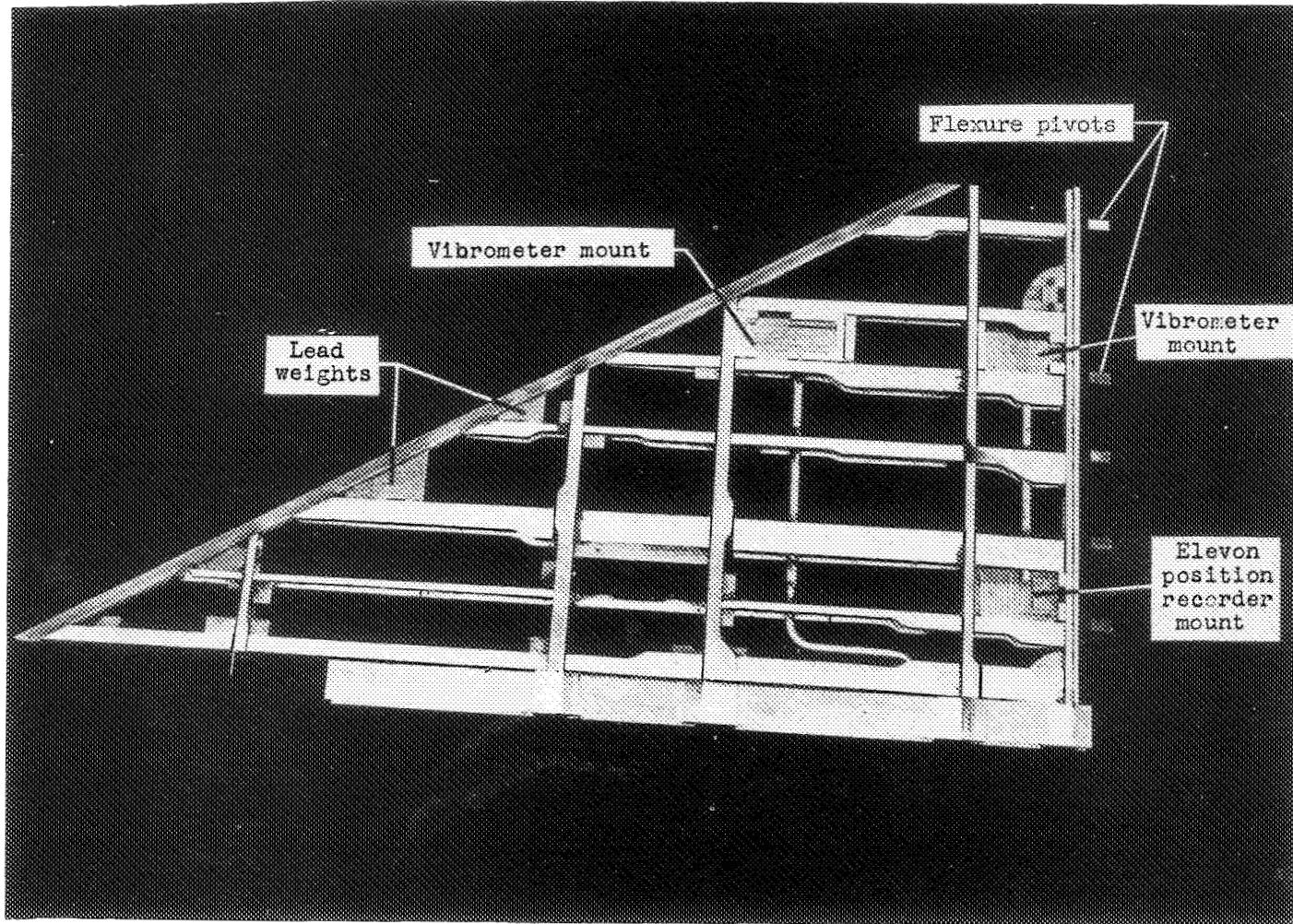
(b) Photograph of wing skeleton.

L-85251.1

Figure 4.- Concluded.

205

118

Vibrometer

144

104

240

81

320

223

320

Elevon position
pick-up
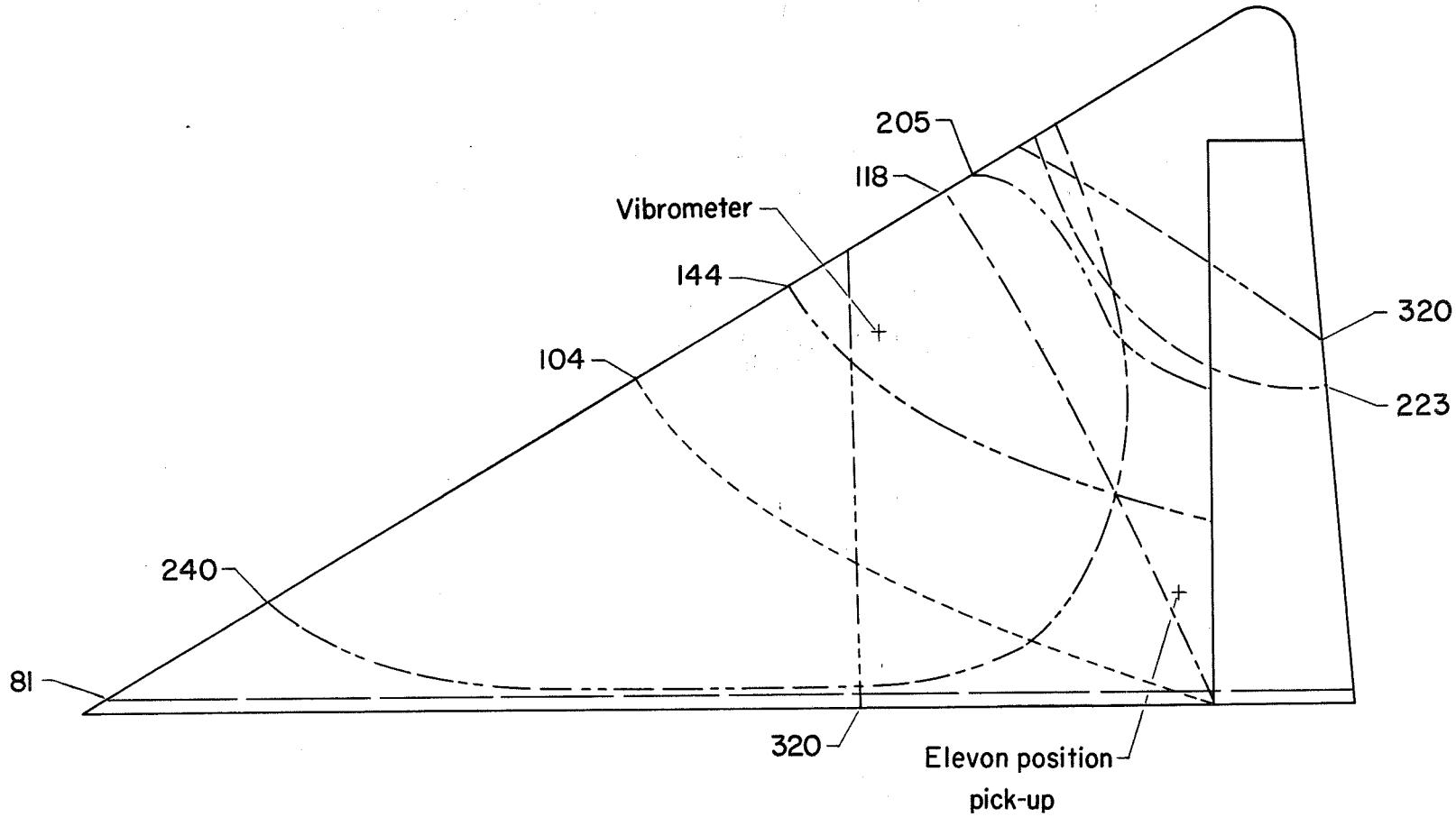
(a) Model 1.

Figure 5.- Node lines and natural frequencies of the wings. Wings and
node line locations are drawn to scale. Frequencies are in cycles
per second.

222

168

Vibrometer

298

100

236

298

76

108 and 124

Elevon position
pick-up

236

298

222
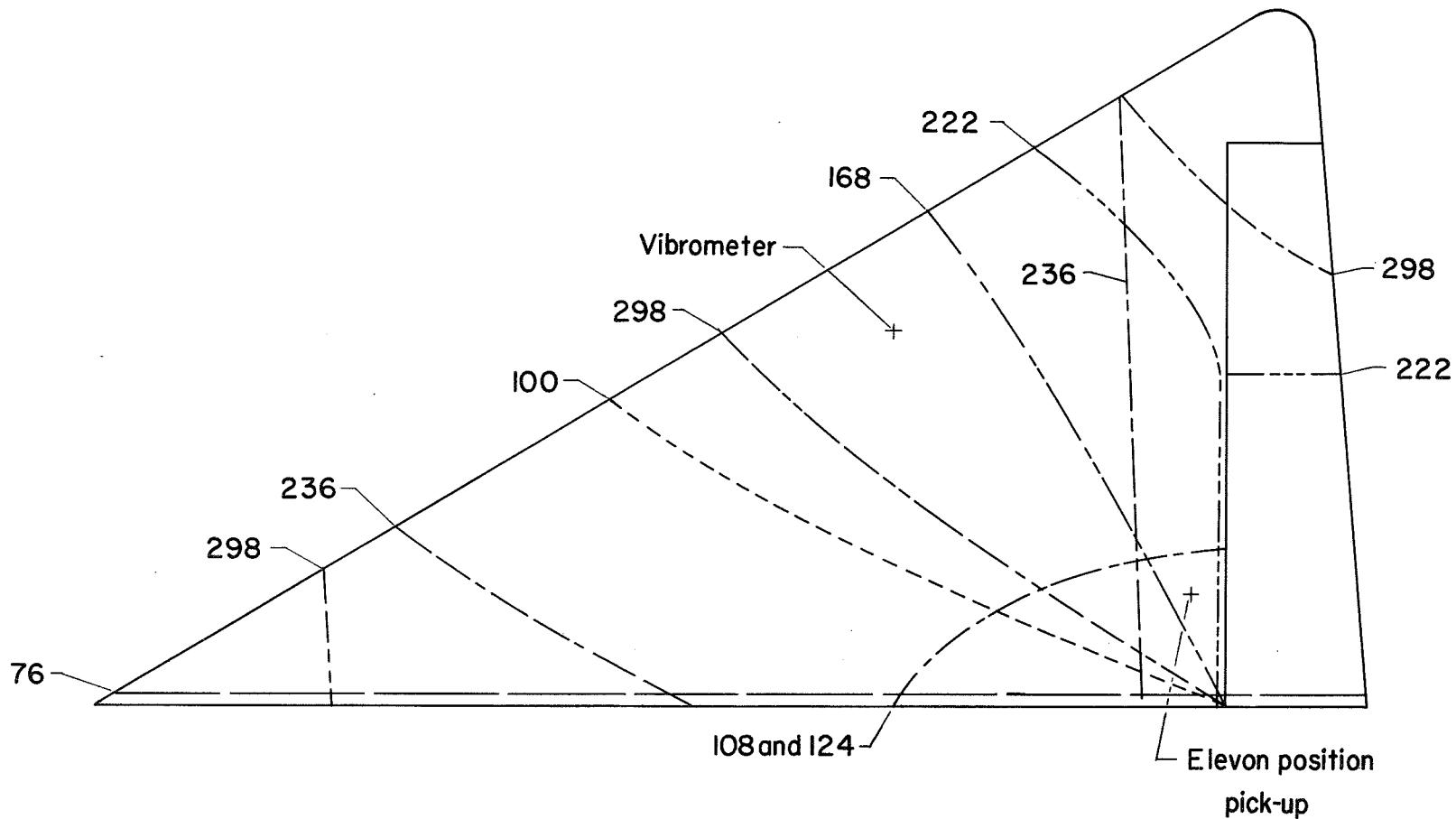
(b) Model 2.

Figure 5.- Concluded.
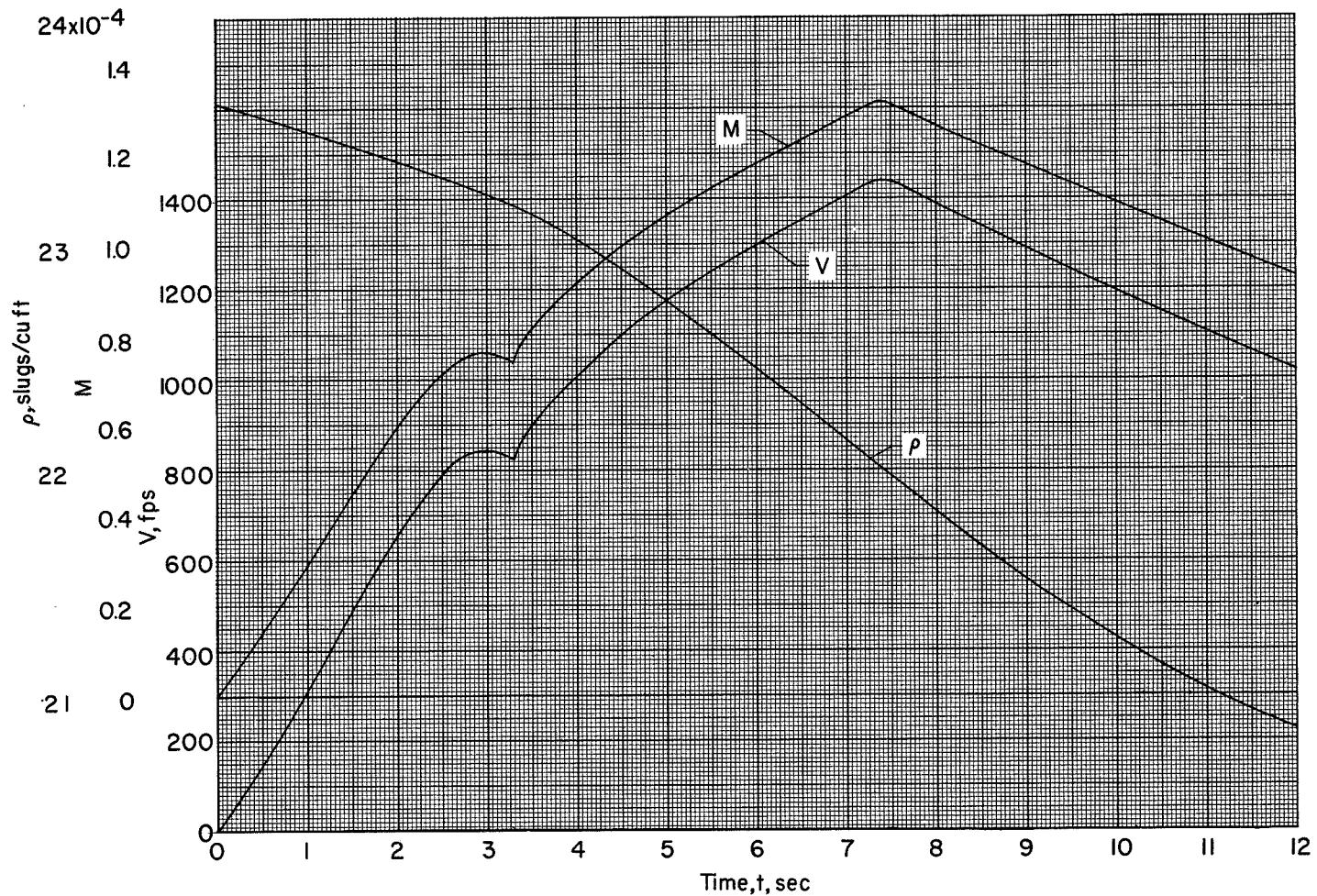
(a) Model 1.

Figure 6.- Time histories showing Mach number, velocity, and atmospheric density.
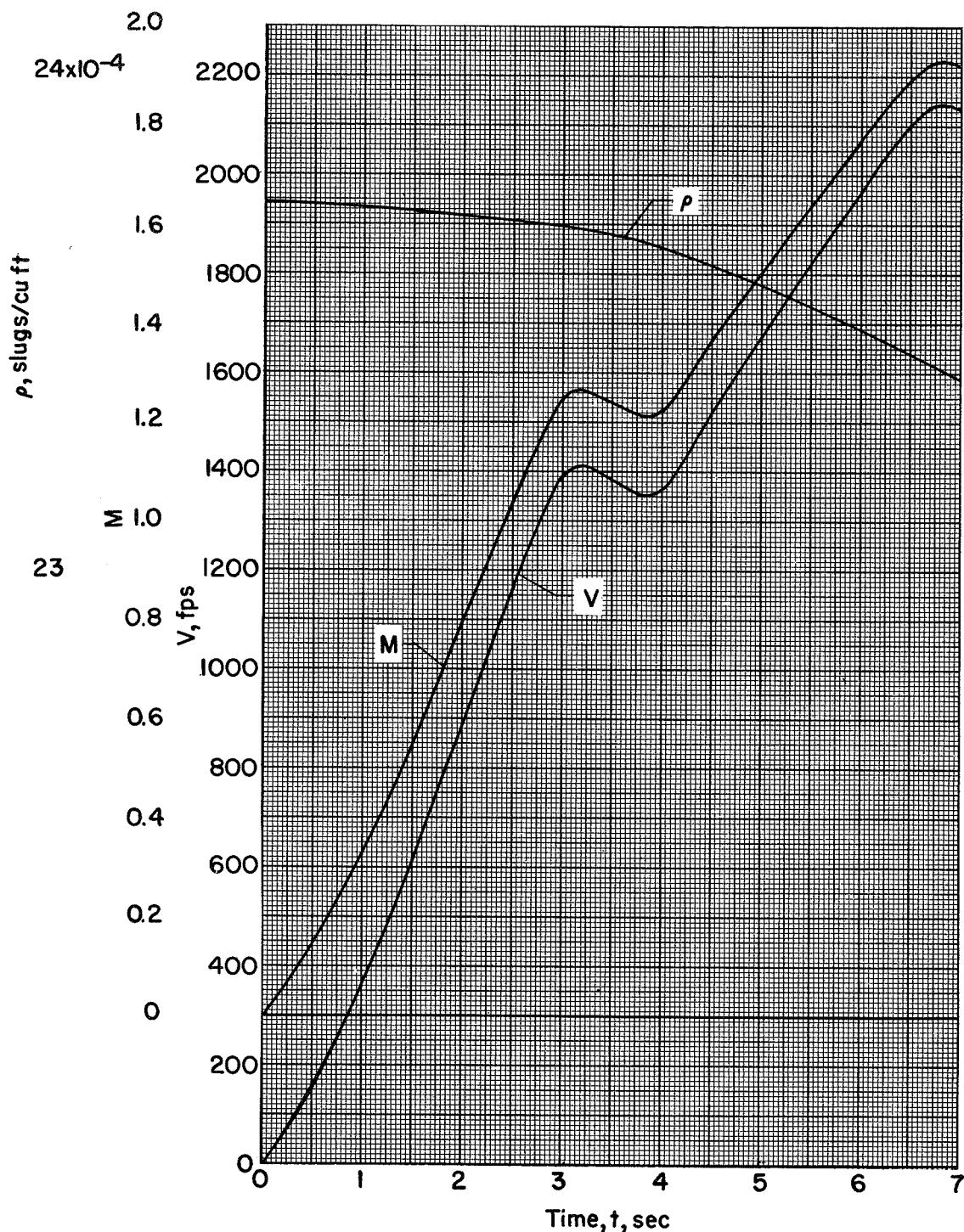
(b) Model 2.

Figure 6.- Concluded.
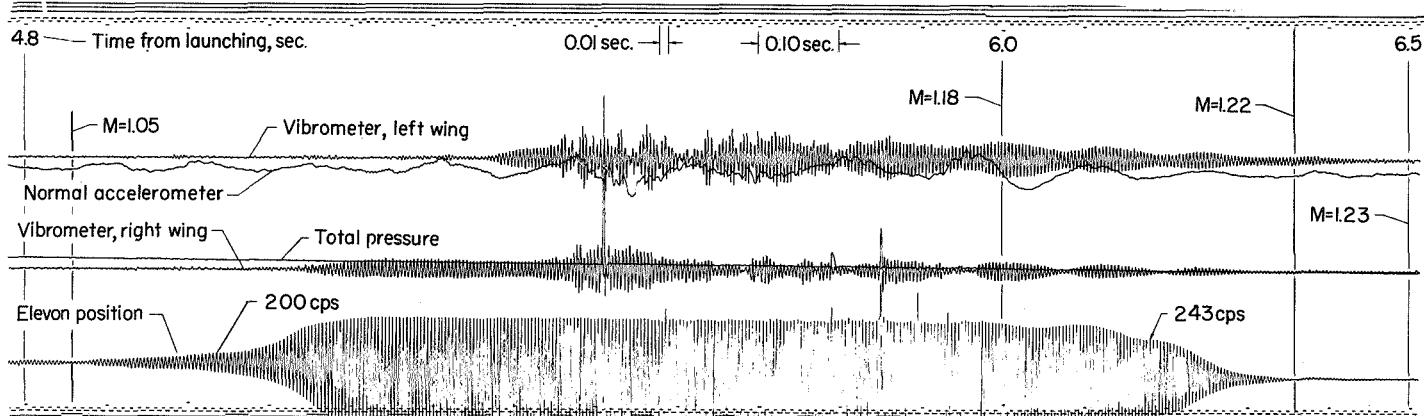
(a) Model 1, accelerating.
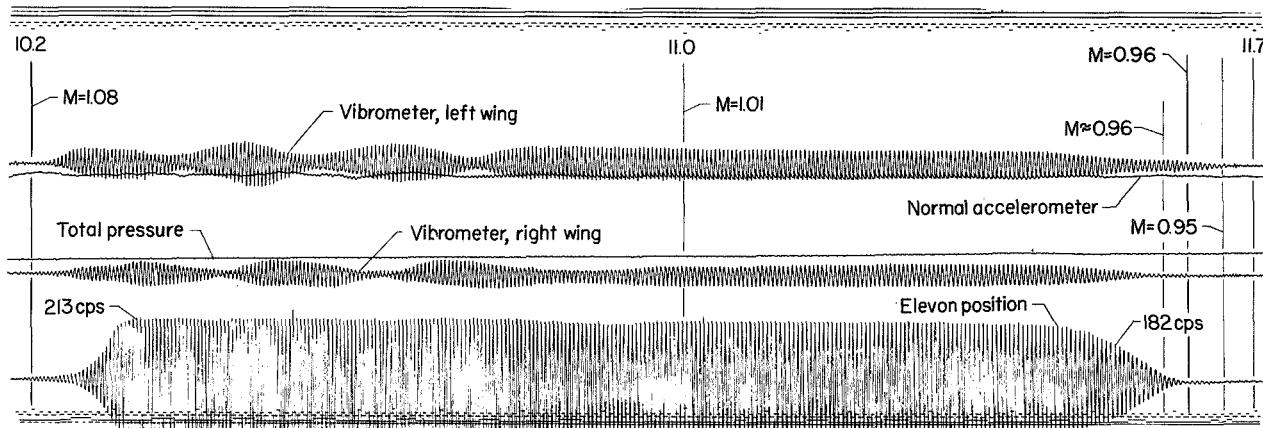


(b) Model 1, coasting.

Figure 7.- Portions of telemeter records.
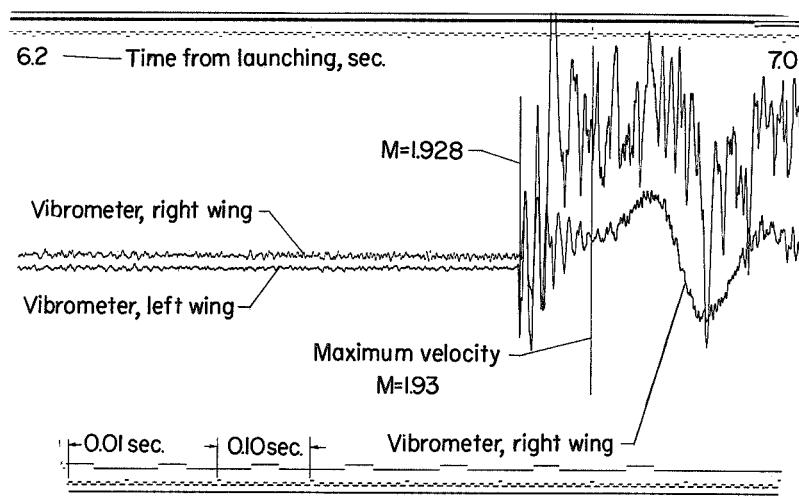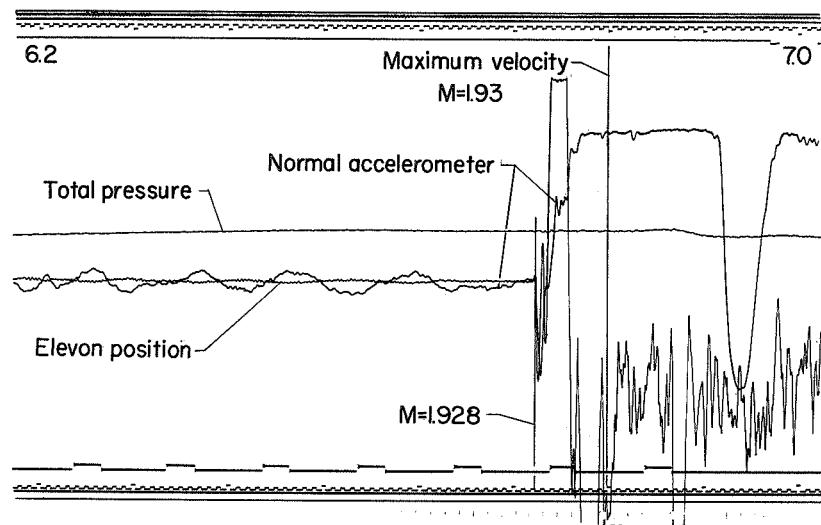
(c) Model 2.

Figure 7.- Concluded.

δ Instrument stop
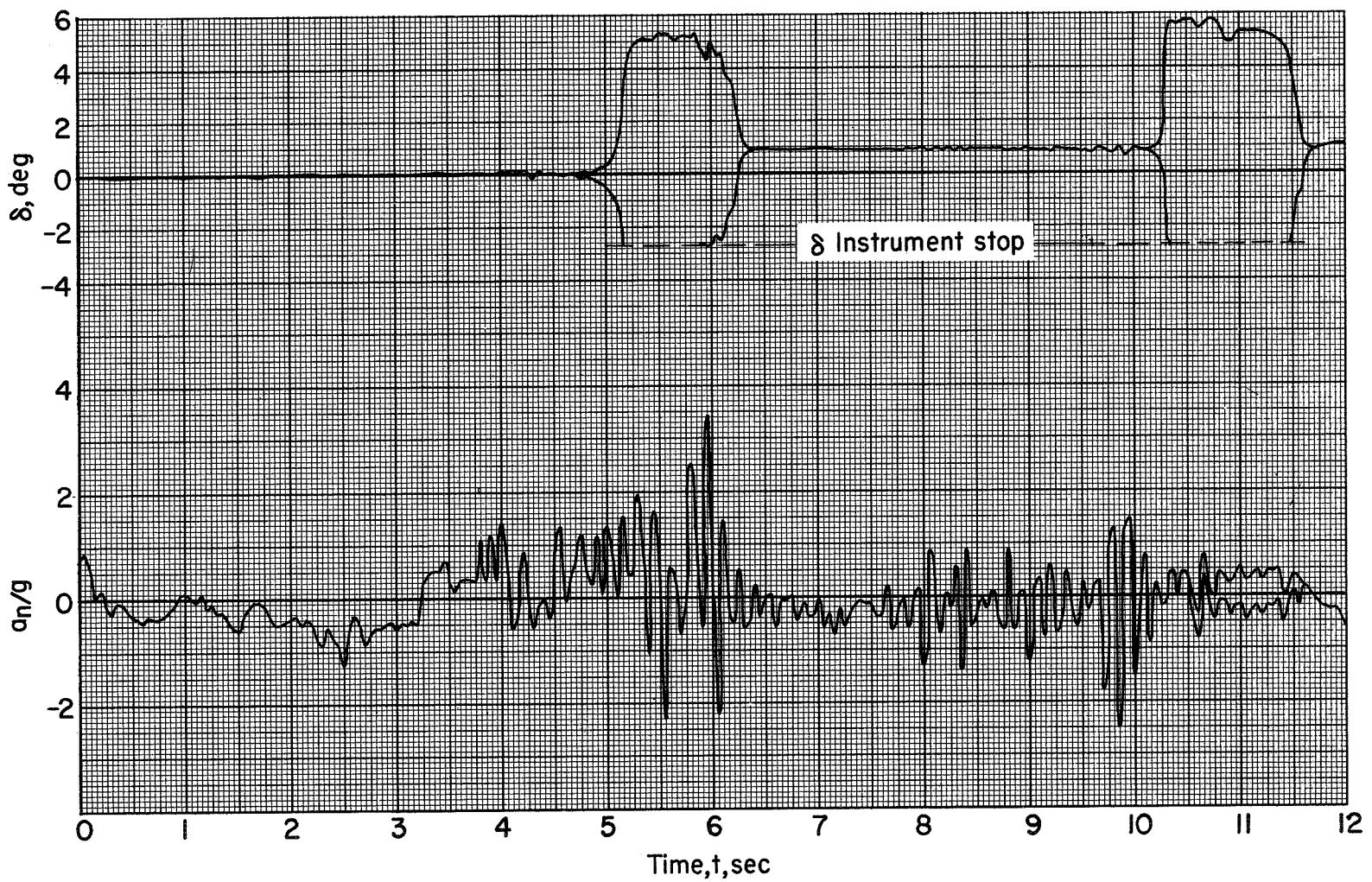
(a) Model 1.

Figure 8.- Reduction of data from telemeter records.
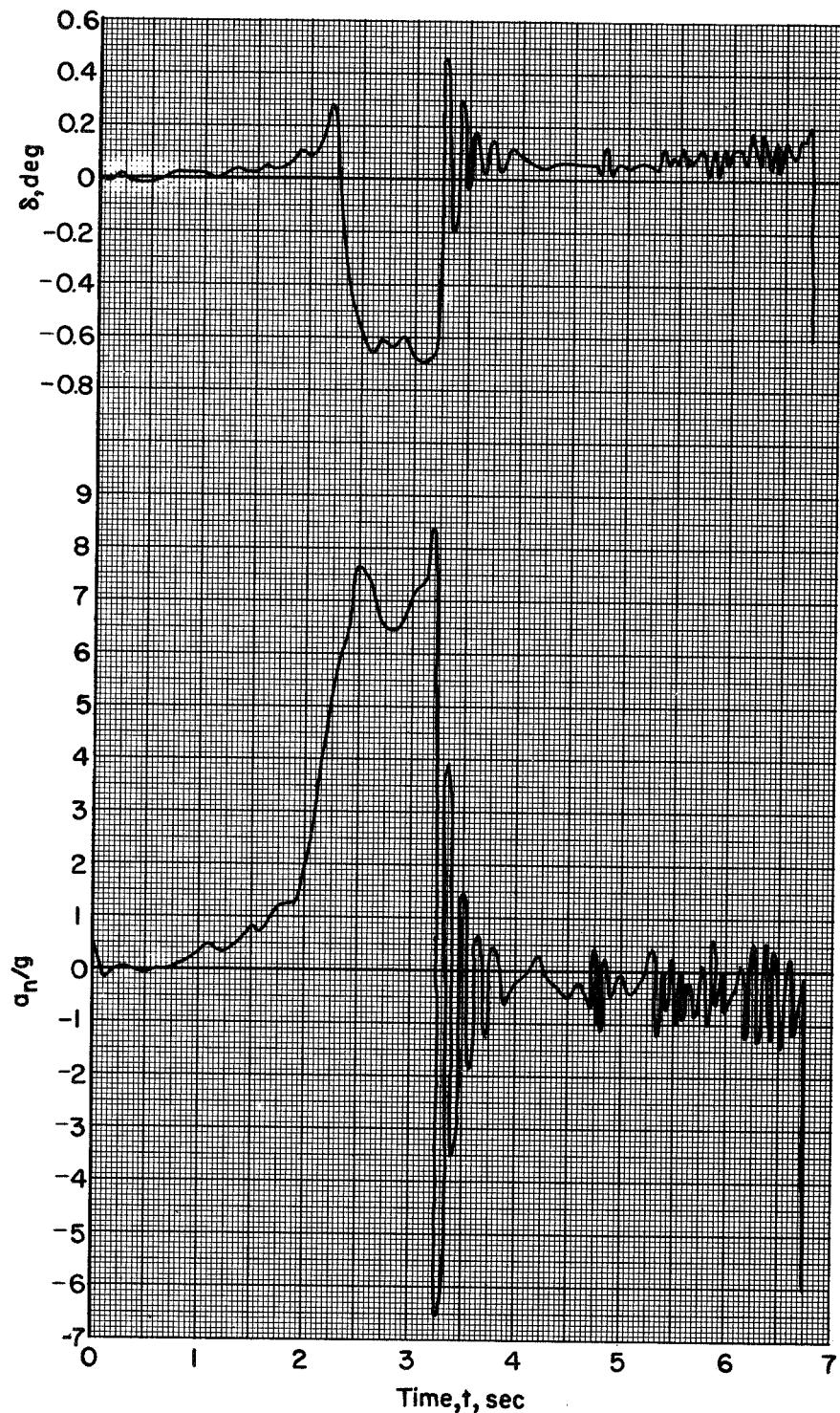
(b) Model 2.

Figure 8.- Concluded.